JOURNAL OF CHEMICAL & ENGINEERING DATA

ARTICLE

pubs.acs.org/jced

Solubility of β-Diketonate Complexes of Copper(II) and Cobalt(II) in Supercritical Carbon Dioxide

Masashi Haruki,* Fumiya Kobayashi, Shin-ichi Kihara, and Shigeki Takishima

Department of Chemical Engineering, Graduate School of Engineering, Hiroshima University, 1-4-1 Kagamiyama, Higashi-Hiroshima 739-8527, Japan

ABSTRACT: The solubilities of the divalent β-diketonate metal complexes, copper(II) and cobalt(II) acetylacetonates ($Cu(acac)_2$ and $Co(acac)_2$), and 2,2,6,6-tetramethyl-3,5-heptanedionates ($Cu(thd)_2$ and $Co(thd)_2$) in supercritical carbon dioxide ($scCO_2$) were measured using a circulation-type apparatus with in situ UV−vis spectrometry at temperatures ranging from (313 to 343) K to accumulate new solubility data on the precursors of conducting and magnetic materials. The solubilities of $Cu(thd)_2$ were about 50- to 65-fold higher than those of $Cu(acac)_2$ at approximately 20 MPa for each temperature level. As for the cobalt complexes, the solubilities of $Co(acac)_2$ were greater than those of $Co(acac)_3$ at 313 K. On the other hand, the solubilities of $Co(thd)_2$ were higher than those of $Co(thd)_3$ in the low CO_2 density region and lower than those of $Co(thd)_3$ in the high CO_2 density region. Moreover, the solubilities of the cobalt complexes were higher than those of the copper complexes for both the metal$(acac)_2$ and metal$(thd)_2$.

INTRODUCTION

Supercritical carbon dioxide ($scCO_2$) is used as a functional and environmentally friendly solvent in many industries, such as food processing, material processing, and the extraction of toxic substances from polluted water or soil. Recently, the application of $scCO_2$ to material processing has received considerable attention due to its superior physical properties, such as a high diffusivity and an ability to control the solubility of solutes through the adjustment of temperature and pressure. For example, in the electronics industry, supercritical fluid deposition can be used to deposit thin films on a surface with a high aspect ratio.[1−3] Moreover, nanocomposite materials, such as engineering polymers with embedded metal compounds, were developed utilizing both the high solubility of the precursor in $scCO_2$ and the plasticization of the polymer due to CO_2 dissolution.[4]

The solubilities of metal complexes that are precursors of metal compounds are critically important data for the design of manufacturing processes, for the molecular design of precursors, and for conducting fundamental research.[5−7] There is a large body of published work regarding the solubility of metal complexes.[8−19] However, only limited kinds of metal complexes have had their solubilities in $scCO_2$ measured before.

Among the many types of metal complexes created for use in many research and industrial fields, hydrocarbon basis β-diketonate complexes, such as metal acetylacetonate (metal$(acac)_n$) and 2,2,6,6-tetramethyl-3,5-heptanedionate (metal$(thd)_n$), are particularly useful because they are fluorine-free and their solubility can be controlled by adjusting the ligand structure. The chemical structures of a metal$(acac)_n$ and a metal$(thd)_n$ are shown in Figure 1. A few research papers have reported the relationship between the chemical structures and the solubilities of β-diketonate complexes.[9,14] Recently, Aschenbrenner et al.[17] investigated the influence of the ligand structure and the types of centered metal on the solubility for mainly metal$(thd)_n$ and metal cyclopentadienyl at only 333 K. They tried to organize the solubilities of metal complexes in $scCO_2$ by the oxidation number and mass number of the centered metal atom, by the melting point of metal complexes, and by using the molecular orbital theory. Many metal complexes were organized well; however, some were not applicable. Therefore, a greater accumulation of systematical data concerning the solubilities of metal complexes is necessary to clarify the relationships between the molecular structure of metal complexes and the solubilities in $scCO_2$. In the present study, the solubilities of copper(II) and cobalt(II) acetylacetonates ($Cu(acac)_2$ and $Co(acac)_2$) and 2,2,6,6-tetramethyl-3,5-heptanedionates ($Cu(thd)_2$ and $Co(thd)_2$) were measured to systematically accumulate solubility data on the precursors of the representative conducting and magnetic materials, respectively, at temperatures ranging from (313 to 343) K.

EXPERIMENTAL SECTION

Materials. Both $Cu(acac)_2$ and $Co(acac)_2$ with purities > 99 % on a weight basis were purchased from Acros Organics Co. $Cu(thd)_2$ and $Co(thd)_2$ with purities > 99.9 % on a weight basis were purchased from Alfa Aesar Co. Benzene of high-performance liquid chromatography (HPLC) grade with a purity > 99.8 mol % was purchased from Nacalai Tesque Co. and was used to prepare the calibration curves. CO_2 with a purity > 99.995 vol % was purchased from Japan Fine Products Co. All materials were used without further purification.

Apparatus and Procedure. A circulation-type apparatus, which was based on the apparatus developed by Carrott and Wai,[20] was used to measure the solubilities of four β-diketonate complexes in $scCO_2$. Since the apparatus was described in detail in previous studies,[21,22] a brief explanation of the experimental apparatus and the procedure is shown here. The apparatus consisted of four main parts: a device used for CO_2 introduction;

Received: November 22, 2010
Accepted: February 16, 2011
Published: March 02, 2011

ACS Publications © 2011 American Chemical Society

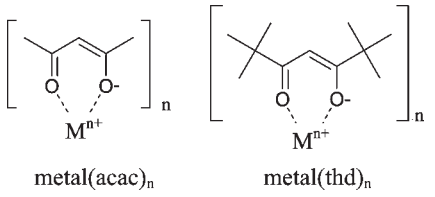

Figure 1. Chemical structure of metal(acac)$_n$ and metal(thd)$_n$.

a circulation assembly located inside a thermostatic air bath (Yamato Scientific Co., DKM300); a multichannel UV−vis spectrometer (Ocean Optics Inc., HR4000 CG-UV-NIR); and a light source (Ocean Optics Inc., DH2000). The circulation assembly consisted of an extraction cell (a stainless steel tube with a diameter of 1/4 in.), a cross-fitting measurement cell (Valco Instrument Co., ZX2L), and a circulation pump (Nihon Seimitsu Kagaku Co., NP-S-461), which were connected by a standard 1/16-in. stainless steel tube. The temperature of the system was measured using a platinum resistance thermometer (JUST Co., TSP type thermometer) connected to an indicator (Shimaden Co., SR94). The head of the thermometer was in contact with the $scCO_2$ that contained a metal complex. The pressure of the system was measured using a pressure transmitter (Huba Control Co., Type-680) connected to a digital indicator (Axis Co., GR3666). The uncertainties of the temperature and pressure measurement were ± 0.3 K and ± 0.005 MPa, respectively. The absorbance of the metal complex in $scCO_2$ was measured at the measurement cell in the circulation loop. The spectrometer and the light source were attached to the measurement cell by optical fibers to perform in situ analyses. The intensity spectrum of transmitted light in pure $scCO_2$ was previously measured at the same temperature and pressure of the solubility measurement as the background spectrum, which was followed by measurement of the $scCO_2$ + metal complex mixture. The absorbance spectrum of the metal complex was obtained from both intensities of the transmitted lights. Two or three measurements were carried out under each set of conditions, and the solubility data were taken from the averages of the measurements.

Calibration Curves. There are reports that the molar extinction coefficient of the solute in $scCO_2$ often depends on the density of $scCO_2$.[23,24] Therefore, the calibration curves used for solubility estimation should be prepared using $scCO_2$ at several temperatures and pressures. However, there are problems associated with preparing a calibration curve with $scCO_2$ using a small volume for the circulation loop because the amount of the metal complex dissolved in $scCO_2$ is often quite small. Instead, in our previous work, the solvent species dependency of the absorbance spectra of the metal complexes in organic solvents and the calibration curves were discussed. Moreover, the solubilities of several kinds of metal complexes estimated based on the calibration curves prepared using the organic solvents were compared with the literature data.[21,22] As a result, there were no noticeable difficulties observed with regard to solubility estimation using a calibration curve prepared with the organic solvents. Therefore, in this work, all four calibration curves used for each metal complex were prepared using benzene at 313 K based on the results of the previous study. In preparation of the calibration curve, the standard solution, which was the solution that contained a given amount of metal complex dissolved in benzene, was introduced into the measurement cell heated at 313 K via HPLC pump. The density of benzene needed to estimate

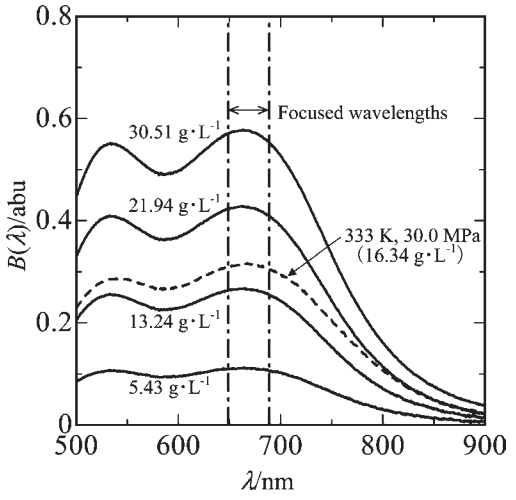

Figure 2. Spectra of Cu(thd)$_2$ in CO_2 and in benzene. —, spectra of Cu(thd)$_2$ in benzene; - - -, spectrum of Cu(thd)$_2$ in CO_2 at 333 K and 30.0 MPa.

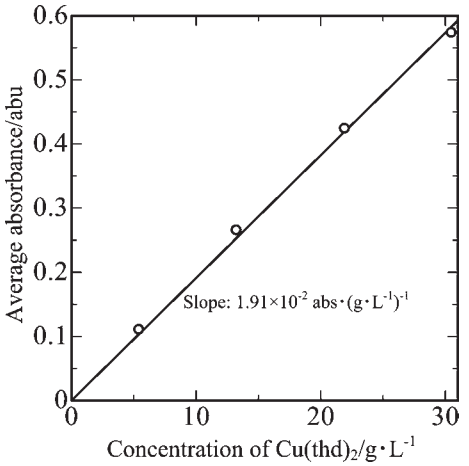

Figure 3. Calibration curve of Cu(thd)$_2$ obtained using benzene as a solvent.

the concentration of the metal complex in the standard solution was obtained from the literature.[25]

The shapes of the spectra for each metal complex in benzene were in good agreement with those in $scCO_2$. As an example, the spectra of Cu(thd)$_2$ in benzene and in $scCO_2$ are shown in Figure 2. Peaks were observed at approximately (533 and 669) nm for benzene and CO_2, respectively. In this study, the spectra of Cu(thd)$_2$ around 669 nm were focused to obtain the solubility. The calibration curves were obtained by using the average absorbance in the vicinity of the focused peak wavelength, as described in eq 1 to reduce the potential deviation based on the small difference in the shape of absorbance spectra and noise in the absorbance data.

$$\text{average absorbance [abu]} = \frac{\int_{\lambda\max-20}^{\lambda\max+20} B(\lambda)\mathrm{d}\lambda}{40} \qquad (1)$$

where λ is the wavelength and the subscripts max+20 and max−20 indicate the wavelengths that were 20 nm away from the peak wavelength. $B(\lambda)$ represents the absorbance of the metal complex at a wavelength of λ. The calibration curve for Cu(thd)$_2$,

Table 1. Experimental Solubility Data for $Cu(acac)_2$ in $scCO_2$

T = 313 K			T = 323 K		
P/MPa	ρ_{CO2}/g·cm^{-3}	$y \cdot 10^5$	P/MPa	ρ_{CO2}/g·cm^{-3}	$y \cdot 10^5$
14.3	0.770	0.997 ± 0.066	15.9	0.721	1.38 ± 0.06
16.1	0.797	1.22 ± 0.05	18.0	0.758	1.51 ± 0.03
18.2	0.823	1.37 ± 0.02	20.1	0.786	1.87 ± 0.01
20.0	0.841	1.50 ± 0.03	22.2	0.809	2.03 ± 0.02
22.1	0.859	1.63 ± 0.04	24.1	0.827	2.25 ± 0.01
24.0	0.873	1.76 ± 0.01	26.0	0.843	2.37 ± 0.01
26.0	0.887	1.81 ± 0.02	27.9	0.857	2.53 ± 0.05
28.1	0.900	1.86 ± 0.04	29.9	0.870	2.69 ± 0.06
30.0	0.910	1.99 ± 0.06			
T = 333 K			T = 343 K		
P/MPa	ρ_{CO2}/g·cm^{-3}	$y \cdot 10^5$	P/MPa	ρ_{CO2}/g·cm^{-3}	$y \cdot 10^5$
16.0	0.639	1.29 ± 0.16	16.1	0.553	1.37 ± 0.10
18.0	0.688	1.82 ± 0.17	18.0	0.613	2.02 ± 0.10
19.9	0.723	2.22 ± 0.12	20.0	0.660	2.72 ± 0.02
22.0	0.753	2.74 ± 0.23	22.1	0.698	3.49 ± 0.14
24.0	0.777	3.05 ± 0.22	24.0	0.725	3.88 ± 0.10
26.0	0.797	3.25 ± 0.09	26.0	0.749	4.48 ± 0.06
27.9	0.814	3.51 ± 0.16	28.0	0.770	4.74 ± 0.10
30.0	0.830	3.87 ± 0.12			

Table 2. Experimental Solubility Data for $Cu(thd)_2$ in $scCO_2$

T = 313 K			T = 323 K		
P/MPa	ρ_{CO2}/g·cm^{-3}	$y \cdot 10^4$	P/MPa	ρ_{CO2}/g·cm^{-3}	$y \cdot 10^4$
11.9	0.716	3.85 ± 0.22	12.2	0.599	2.71 ± 0.09
14.1	0.766	5.65 ± 0.02	14.1	0.677	5.47 ± 0.25
15.9	0.795	5.97 ± 0.10	15.9	0.721	6.50 ± 0.57
18.0	0.820	7.07 ± 0.01	18.0	0.758	8.90 ± 0.46
20.0	0.841	7.55 ± 0.02	20.2	0.788	10.3 ± 0.7
22.0	0.858	8.13 ± 0.05	22.0	0.807	11.7 ± 0.8
24.1	0.874	8.40 ± 0.03	23.9	0.825	12.5 ± 0.5
26.0	0.887	8.57 ± 0.06	26.1	0.844	13.5 ± 0.1
			28.0	0.858	13.8 ± 0.2
T = 333 K			T = 343 K		
P/MPa	ρ_{CO2}/g·cm^{-3}	$y \cdot 10^4$	P/MPa	ρ_{CO2}/g·cm^{-3}	$y \cdot 10^4$
14.0	0.563	4.00 ± 0.07	14.1	0.463	2.80 ± 0.51
16.0	0.639	7.31 ± 0.11	16.0	0.549	7.05 ± 0.48
18.0	0.688	11.2 ± 0.1	18.0	0.613	11.8 ± 0.3
20.2	0.728	13.4 ± 0.9	20.0	0.660	17.4 ± 0.4
22.0	0.753	15.4 ± 1.3	22.0	0.696	22.3 ± 0.7
24.0	0.777	17.3 ± 1.4	24.1	0.726	26.8 ± 0.3
26.0	0.797	18.9 ± 0.7	26.1	0.750	29.4 ± 1.0
28.1	0.815	20.3 ± 0.2	28.0	0.770	32.0 ± 0.4
30.0	0.830	21.1 ± 0.5	30.2	0.790	33.9 ± 1.1

which represents the relationship between the concentration of $Cu(thd)_2$ in benzene and the average absorbance, is shown in Figure 3. A linear relationship based on Lambert−Beer's law was

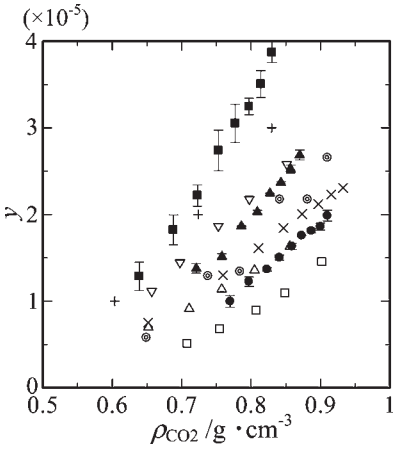

Figure 4. Experimental solubilities of $Cu(acac)_2$ in $scCO_2$. ●, ▲, ■, this work at (313, 323, and 333) K; ×, Lagalante et al.[9] at 313.15 K; ⊙, Yoda et al.[18] at 313 K; +, Aschenbrenner et al.[17] at 333 K; □, △, ▽, Cross et al.[10] at (308.15, 318.15, and 328.15) K.

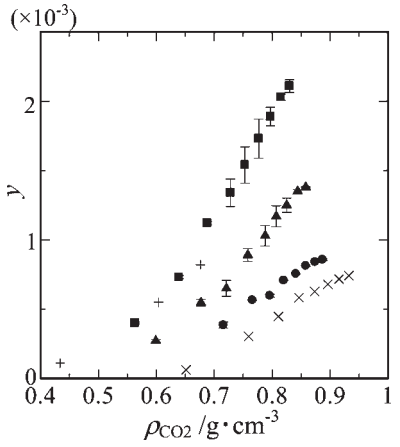

Figure 5. Experimental solubilities of $Cu(thd)_2$ in $scCO_2$. ●, ▲, ■, this work at (313, 323, and 333) K; × , Lagalante et al.[9] at 313.15 K; +, Aschenbrenner et al.[17] at 333 K.

obtained. The calibration curves of $Cu(acac)_2$, $Co(acac)_2$, and $Co(thd)_2$ were also prepared using the same procedure as for $Cu(thd)_2$. The focused peak wavelengths were 669, 557, and 557 nm for $Cu(acac)_2$, $Co(acac)_2$, and $Co(thd)_2$, respectively, and linear relationships were also obtained for the concentration of the metal complex in benzene and the average absorbance for all metal complexes.

RESULTS AND DISCUSSION

Experimental results for the solubilities of $Cu(acac)_2$ and $Cu(thd)_2$ in $scCO_2$ at temperatures ranging from (313 to 343) K are listed in Tables 1 and 2, respectively, along with their standard deviations. The CO_2 densities were obtained using the Span−Wagner equation of state[26] for each condition. The experimental results of $Cu(acac)_2$ and $Cu(thd)_2$ are also described in Figures 4 and 5, respectively, along with the experimental solubilities reported in the literature. As for the $Cu(acac)_2$, the experimental solubilities at 313 K were compared with the data of Lagalante et al.[9] and Yoda et al.[18] An in situ spectrometric analysis similar to that used in the present work and an HPLC analysis were used for solubility measurements by

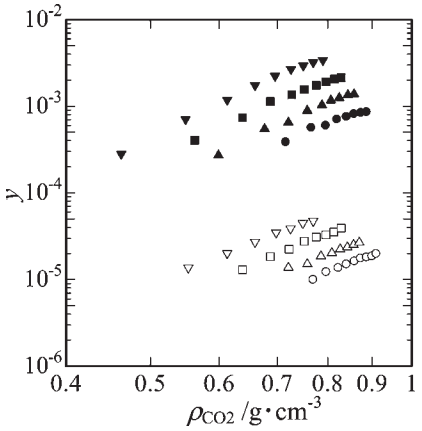

Figure 6. Comparison of solubilities of copper complexes in $scCO_2$. ○, △, □, ▽, $Cu(acac)_2$ at (313, 323, 333, and 343) K; ●, ▲, ■, ▼, $Cu(thd)_2$ at (313, 323, 333, and 343) K.

Table 3. Experimental Solubility Data for $Co(acac)_2$ in $scCO_2$

T = 313 K		
P/MPa	ρ_{CO2}/g·cm^{-3}	$y \cdot 10^5$
16.1	0.797	3.91 ± 0.79
18.0	0.820	4.82 ± 0.07
20.1	0.842	5.94 ± 0.51
21.9	0.857	6.50 ± 0.04
24.0	0.873	6.99 ± 0.09
25.9	0.886	7.38 ± 0.01
28.1	0.900	8.24 ± 0.19
30.0	0.910	8.59 ± 1.13

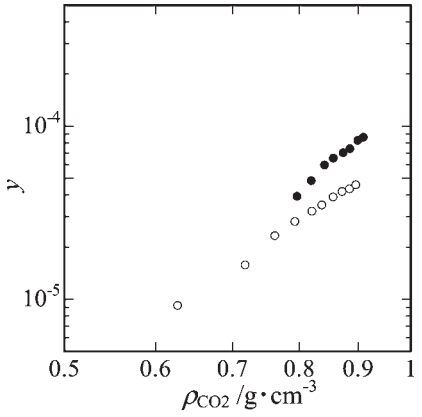

Figure 7. Experimental solubilities of $Co(acac)_n$ complexes in $scCO_2$. ●, $Co(acac)_2$ at 313 K; ○, literature data[21] for $Co(acac)_3$ at 313 K.

Lagalante et al. and Yoda et al., respectively. The data measured in the present work were slightly low compared with the data reported in those two studies. The average absolute relative deviations (AARDs) between the isothermal curves of the present work and that of the literature data were 21 % and 31 %, respectively. On the other hand, the data from the present study were in good agreement with the data measured using the semibatch flow method with gravimetric analysis by Aschenbrenner et al.[17] at 333 K, with the exception of the data

Table 4. Experimental Solubility Data for $Co(thd)_2$ in $scCO_2$

T = 313 K			T = 323 K		
P/MPa	ρ_{CO2}/g·cm^{-3}	$y \cdot 10^4$	P/MPa	ρ_{CO2}/g·cm^{-3}	$y \cdot 10^4$
10.0	0.632	4.60 ± 0.01	10.4	0.436	2.10 ± 0.06
10.9	0.681	6.20 ± 0.05	11.1	0.516	3.65 ± 0.25
11.9	0.716	7.29 ± 0.05	12.0	0.587	5.77 ± 0.10
13.0	0.744	7.74 ± 0.56	13.0	0.638	7.43 ± 0.01
14.0	0.764	8.54 ± 0.39	14.0	0.674	8.39 ± 0.24
15.0	0.781	8.85 ± 0.88	15.0	0.701	9.63 ± 0.32
16.0	0.796	9.06 ± 1.24	16.0	0.723	10.5 ± 0.2
17.0	0.809	9.72 ± 0.90	17.0	0.742	11.2 ± 0.1
T = 333 K			T = 343 K		
P/MPa	ρ_{CO2}/g·cm^{-3}	$y \cdot 10^4$	P/MPa	ρ_{CO2}/g·cm^{-3}	$y \cdot 10^4$
10.0	0.291	0.795 ± 0.092	10.9	0.290	1.20 ± 0.28
11.1	0.367	1.78 ± 0.38	12.0	0.347	2.31 ± 0.51
12.0	0.436	3.42 ± 0.25	13.0	0.403	3.98 ± 0.47
13.0	0.507	5.87 ± 0.09	14.0	0.458	6.33 ± 0.33
13.9	0.558	8.10 ± 0.28	15.0	0.507	9.51 ± 0.46
14.9	0.602	11.3 ± 0.2	15.9	0.545	12.3 ± 1.1
15.9	0.636	12.8 ± 0.4			

at about 0.83 g·cm^{-3} of CO_2 density. Cross et al.[10] also measured the solubilities of $Cu(acac)_2$ in a range from (308.15 to 328.15) K using the semibatch flow method, and the slope of isothermal solubility curves of the present work were slight different, although the deviations between the solubilities of the present work and that of Cross et al. were not large. As for the solubilities of $Cu(thd)_2$, as described in Figure 5, the solubilities of the present work were higher than those measured by Lagalante et al.[9] contrary to the results of $Cu(acac)_2$ at 313 K. The AARD between the solubilities of the present work and that of Lagalante et al. was 31 %. However, the solubilities of the present work agreed with that of Aschenbrenner et al.[17] at 333 K. Overall, the data from the present work agreed with the literature data regardless of the differences in measurement methods.

Moreover, the relationship between the solubilities of $Cu(acac)_2$ and $Cu(thd)_2$ is illustrated on the double logarithmic chart in Figure 6. Approximately linear relationships were obtained for the isothermal solubility curves of both copper complexes, and the slopes of the isothermal curves were nearly identical. The solubilities of $Cu(thd)_2$ were approximately 50- to 65-fold higher than those of $Cu(acac)_2$ at around 20 MPa for each temperature level. One explanation for this experimental result is that the ligands of $Cu(thd)_2$ more thoroughly covered the centered copper atom compared with those of $Cu(acac)_2$, as well as cobalt(III), and chromium(III) complexes, as reported in previous work.[22]

The experimental solubilities of $Co(acac)_2$ in $scCO_2$ at 313 K are listed in Table 3 and described in Figure 7 along with the data of $Co(acac)_3$, as measured in previous work.[21] As shown in the figure, the solubilities of $Co(acac)_2$ were approximately 1.4- to 1.8-fold higher than those of $Co(acac)_3$ at each CO_2 density level. Moreover, the solubilities of $Co(thd)_2$ at temperatures ranging from (313 to 343) K are listed in Table 4 and shown in Figure 8 along with the results of $Co(thd)_3$.[22] Linear relationships were also obtained for each isothermal solubility curve, as described in Figure 8, although the slopes of each isothermal

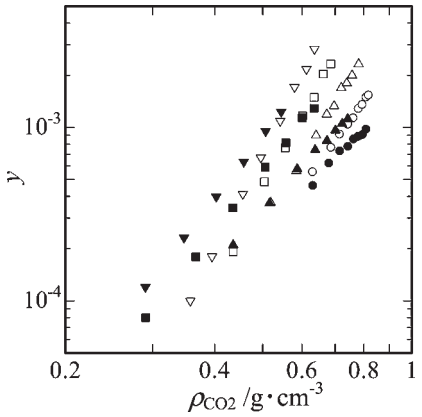

Figure 8. Experimental solubilities of $Co(thd)_n$ complexes in $scCO_2$. ●, ▲, ■, ▼, $Co(thd)_2$ at (313, 323, 333, and 343) K; ○, △, □, ▽, literature data[22] for $Co(thd)_3$ at (313, 323, 333, and 343) K.

curve were slightly different, and the solubility of $Co(thd)_2$ was about 23-fold higher than that of $Co(acac)_2$ at 16 MPa and 313 K. On the other hand, solubilities of $Co(thd)_2$ were higher than those of $Co(thd)_3$ in the low CO_2 density region and lower than those of $Co(thd)_3$ in the high CO_2 density region as shown in Figure 8 because the CO_2 density dependencies of the isothermal solubility curves for $Co(thd)_2$ were different from those for $Co(thd)_3$. This relationship was different from the relationship between $Co(acac)_2$ and $Co(acac)_3$. Namely, the effect of the valence of the centered metal on the solubility of the metal complex in $scCO_2$ depended on the ligand structure, which is considered to be caused by a difference in shielding effects based on the ligand structure.

Furthermore, the solubilities of $Co(acac)_2$ and $Co(thd)_2$ were higher than those of $Cu(acac)_2$ and $Cu(thd)_2$, respectively. In the study by Aschenbrenner et al.,[17] the solubility difference caused by the differences in centered metal were discussed by the melting temperature related to the cohesive energy and by the distance between the centered metal and the ligand related to the shielding effect by the ligands. According to the material safety data sheets from the supplier of each metal complex used in this work, the melting points are (438 to 443) K for $Co(acac)_2$, 518 K for $Cu(acac)_2$, 416 K for $Co(thd)_2$, and 471 K for $Cu(thd)_2$, respectively. Therefore, the cohesive energies of $Co(acac)_2$ and $Co(thd)_2$ are expected to be smaller than those of $Cu(acac)_2$ and $Co(thd)_2$, which may be one of the reasons for differences between the solubilities of the cobalt complexes and the copper complexes.

CONCLUSIONS

In the present study, the solubilities of the β-diketonate complexes of copper(II) and cobalt(II), such as $Cu(acac)_2$, $Cu(thd)_2$, $Co(acac)_2$, and $Co(thd)_2$ in $scCO_2$, were measured at temperatures ranging from (313 to 343) K using a circulation-type apparatus with in situ UV−vis spectrometric analysis. The solubilities of $Cu(acac)_2$ and $Cu(thd)_2$ approximately corresponded to the literature data, and the solubilities of $Cu(thd)_2$ were about 50- to 65-fold higher than those of $Cu(acac)_2$ at about 20 MPa for each temperature level. As for the cobalt complexes, the solubilities of $Co(acac)_2$ were greater than those of $Co(acac)_3$. On the other hand, the solubilities of $Co(thd)_2$ were higher than those of $Co(thd)_3$ in the low CO_2 density region and lower than those of $Co(thd)_3$ in the high CO_2 density region, respectively. Moreover, the solubilities of $Co(acac)_2$ and $Co(thd)_2$ were higher than those of $Cu(acac)_2$ and $Cu(thd)_2$, respectively.

AUTHOR INFORMATION

Corresponding Author

*Tel.: +81-82-424-7713. Fax: +81-82-424-7713. E-mail: mharuki@hiroshima-u.ac.jp.

REFERENCES

(1) Kondoh, E. Deposition of Cu and Ru thin films in deep nanotrenches/holes using supercritical carbon dioxide. *Jpn. J. Appl. Phys.* **2004**, *43*, 3928–3933.

(2) Zong, Y.; Watkins, J. J. Deposition of copper by the H_2-assisted reduction of $Cu(tmod)_2$ in supercritical carbon dioxide:kinetics and reaction mechanism. *Chem. Mater.* **2005**, *17*, 560–565.

(3) Kondoh, E.; Fukuda, J. Deposition kinetics and narrow-gap-filling in Cu thin film growth from supercritical carbon dioxide fluids. *J. Supercrit. Fluids* **2008**, *44*, 466–474.

(4) Yoda, S.; Hasegawa, A.; Suda, H.; Uchimaru, Y.; Haraya, K.; Tsuji, T.; Otake, K. Preparation of a platinum and palladium/polyimide nanocomposite film as a precursor of metal-doped carbon molecular sieve membrane via supercritical impregnation. *Chem. Mater.* **2004**, *16*, 2363–2368.

(5) de Dea, S.; Graziani, D.; Miller, D. R.; Continetti, R. E. Growth of magnetic thin films using CO_2 RESS expansions. *J. Supercrit. Fluids* **2007**, *42*, 410–418.

(6) Puniredd, S. R.; Weiyi, S; Srinivasan, M. P. Pd−Pt and Fe−Ni nanoparticles formed by covalent molecular assembly in supercritical carbon dioxide. *J. Colloid Interface Sci.* **2008**, *329*, 333–340.

(7) Chen, Z.; Zhuo, M.; Xue, F.; Chen, J.; Xu, Q. Preparation of magnetically separable mesoporous silica microspheres with open pore systems in supercritical carbon dioxide. *Ind. Eng. Chem. Res.* **2009**, *48*, 3441–3445.

(8) Saito, N.; Ikushima, Y.; Goto, T. Liquid/solid extraction of acetylacetone chelates with supercritical carbon dioxide. *Bull. Chem. Soc. Jpn.* **1990**, *63*, 1532–1534.

(9) Lagalante, A. F.; Hansen, B. N.; Bruno, T. J.; Sievers, R. E. Solubilities of copper(II) and chromium(III) β-diketonates in supercritical carbon dioxide. *Inorg. Chem.* **1995**, *34*, 5781–5785.

(10) Cross, W., Jr.; Akgerman, A.; Erkey, C. Determination of metal-chelate complex solubilities in supercritical carbon dioxide. *Ind. Eng. Chem. Res.* **1996**, *35*, 1765–1770.

(11) Smart, N. G.; Carleson, T.; Kast, T.; Clifford, A. A.; Burford, M. D.; Wai, C. M. Solubility of chelating agents and metal-containing compounds in supercritical fluid carbon dioxide. *Talanta* **1997**, *44*, 137–150.

(12) Özel, M. Z.; Bartle, K. D.; Clifford, A. A.; Burford, M. D. Extraction, solubility and stability of metal complexes using stainless steel supercritical fluid extraction system. *Anal. Chim. Acta* **2000**, *417*, 177–184.

(13) Roggeman, S. J.; Scurto, A. M.; Brennecke, J. F. Spectroscopy, solubility, and modeling of cosolvent effects on metal chelate complexes in supercritical carbon dioxide solutions. *Ind. Eng. Chem. Res.* **2001**, *40*, 980–989.

(14) Andersen, W. C.; Sievers, R. E.; Lagalante, A. F.; Bruno, T. J. Solubilities of cerium(IV), terbium(III), and iron(III) β-diketonates in supercritical carbon dioxide. *J. Chem. Eng. Data* **2001**, *46*, 1045–1049.

(15) Guigard, S. E.; Hayward, G. L.; Zytner, R. G.; Stiver, W. H. Measurement of solubilities in supercritical fluids using a piezoelectric quartz crystal. *Fluid Phase Equilib.* **2001**, *187−188*, 233–246.

(16) Ohashi, A.; Hoshino, H.; Niida, J.; Imura, H.; Ohashi, K. Remarkable enhancement effect of 2,2,2-trifluoroethanol on the solubility of tris (pentane-2,4-dionato) chromium(III) in supercritical carbon dioxide by outer-sphere complexation through hydrogen bonding. *Bull. Chem. Soc. Jpn.* **2005**, *78*, 1804–1809.

(17) Aschenbrenner, O.; Kemper, S.; Dahmen, N.; Schaber, K.; Dinjus, E. Solubility of β -diketonates, cyclopentadienyls, and cyclooctadiene complexes with various metals in supercritical carbon dioxide. *J. Supercrit. Fluids* **2007**, *41*, 179–186.

(18) Yoda, S.; Mizuno, Y.; Furuya, T.; Takebayashi, Y.; Otake, K.; Tsuji, T.; Hiaki, T. Solubility measurements of noble metal acetylacetonates in supercritical carbon dioxide by high performance liquid chromatography (HPLC). *J. Supercrit. Fluids* **2008**, *44*, 139–147.

(19) Gupta, R. B.; Shim, J. J. *Solubility in Supercritical Carbon Dioxide*; CRC Press Taylor & Francis Group: Boca Raton, 2007.

(20) Carrott, M. J.; Wai, C. M. UV-visible spectroscopic measurement of solubilities in supercritical CO_2 using high-pressure fiber-optic cells. *Anal. Chem.* **1998**, *70*, 2421–2425.

(21) Haruki, M.; Kobayashi, F.; Kishimoto, K.; Kihara, S.; Takishima, S. Measurement of the solubility of metal complexes in supercritical carbon dioxide using a UV−vis spectrometer. *Fluid Phase Equilib.* **2009**, *280*, 49–55.

(22) Haruki, M.; Kobayashi, F.; Okamoto, M.; Kihara, S.; Takishima, S. Solubility of β-diketonate complexes for cobalt(III) and chromium-(III) in supercritical carbon dioxide. *Fluid Phase Equilib.* **2010**, *297*, 155–161.

(23) Inomata, H.; Yagi, Y.; Saito, M.; Saito, S. Density dependence of the molar absorption coefficient −Application of the Beer-Lambert law to supercritical CO_2-naphthalene mixture. *J. Supercrit. Fluids* **1993**, *6*, 237–240.

(24) Rice, J. K.; Niemeyer, E. D.; Bright, F. V. Evidence for density-dependent changes in solute molar absorptivities in supercritical CO_2: Impact on solubility determination practices. *Anal. Chem.* **1995**, *67*, 4354–4357.

(25) Vargaftik, N. B.; Vinogradov, Y. K.; Yargin, V. S. *Handbook of Physical Properties of Liquids and Gases−Pure Substances and Mixtures*, 3rd Augmented and Revised ed.; Begell House, Inc.: New York, 1996.

(26) Span, R.; Wagner, W. A new equation of state for carbon dioxide covering the fluid region from the triple-point temperature to 1100 K at pressures up to 800 MPa. *J. Phys. Chem. Ref. Data* **1996**, *25*, 1509–1596.